# Supporting Information

# Luminescence modulation in liquid crystalline phases containing a dispiro[fluorene-9,11'-indeno[1,2-*b*]fluorene-12',9''-fluorene] core

Sébastien Thiery,[a] Benoît Heinrich,[b] Bertrand Donnio,[b,c,*] Cyril Poriel[a,*] and Franck Camerel[a,*]

[a] Institut des Sciences Chimiques de Rennes, UMR 6226 (CNRS-Université de Rennes 1), Campus de Beaulieu, 35042 Rennes, France.

E-mail: cyril.poriel@univ-rennes1.fr; franck.camerel@univ-rennes1.fr

[b] Institut de Physique et Chimie des Matériaux de Strasbourg (IPCMS), UMR 7504 (CNRS-Université de Strasbourg), 23 rue du Loess, BP 43, 67034 Strasbourg Cedex 2, France.

[c] Complex Assemblies of Soft Matter Laboratory (COMPASS), UMI 3254 (CNRS-Rhodia/Solvay-University of Pennsylvania), CRTB, 350 George Patterson Boulevard, Bristol, PA 19007, USA.

Email : bdonnio@ipcms.unistra.fr

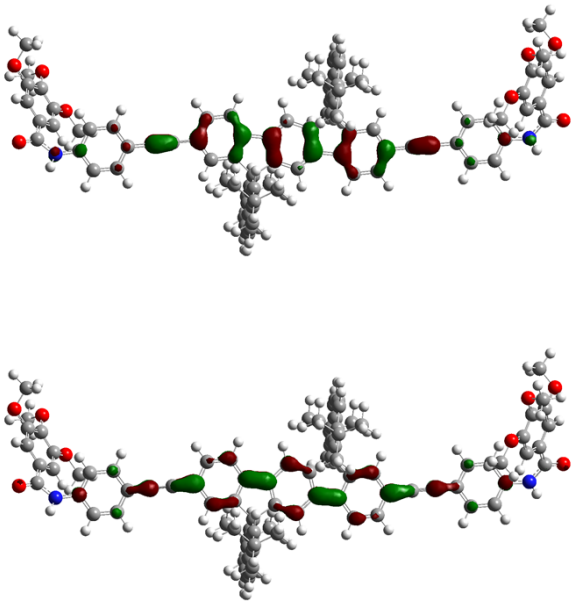

**Figure S1**. Sketch of frontier molecular orbitals (from DFT calculations) for a simplified model of **1** (methyl instead of hexadecyl groups, Highest Occupied Molecular Orbital, HOMO, (top) and Lowest Unoccupied Molecular Orbital, LUMO, (bottom)

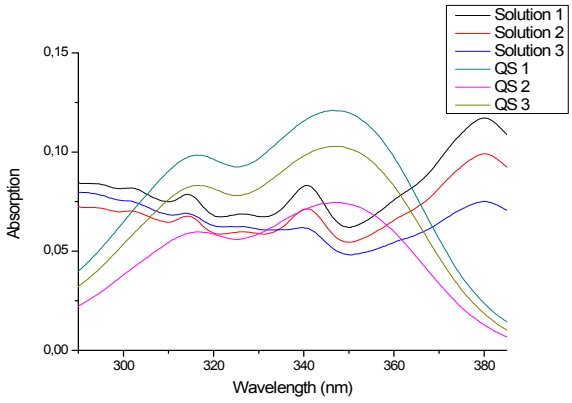


**Figure S2.** Quantum yield measurements : Absorption of solutions of **1** and quinine sulfate (QS) in dichloromethane.

**Table S1.** Quantum yield calculation of **1**

| Solution | λ (nm) | A | $T_S$ | $T_{QS}$ | $n_D^{25}$ (dichloromethane) | $n_D^{25}$ ($H_2SO_4$ 1N) | ϕ |
|---|---|---|---|---|---|---|---|
| 1 | 306 | 0.079 | 56926.3 | 110896 | 1.421 | 1.3325 | 32% |
| 2 | 358 | 0.0627 | 73235.7 | 137327 | 1.421 | 1.3325 | 33% |
| 3 | 366.5 | 0.0596 | 64810.6 | 129041 | 1.421 | 1.3325 | 31% |

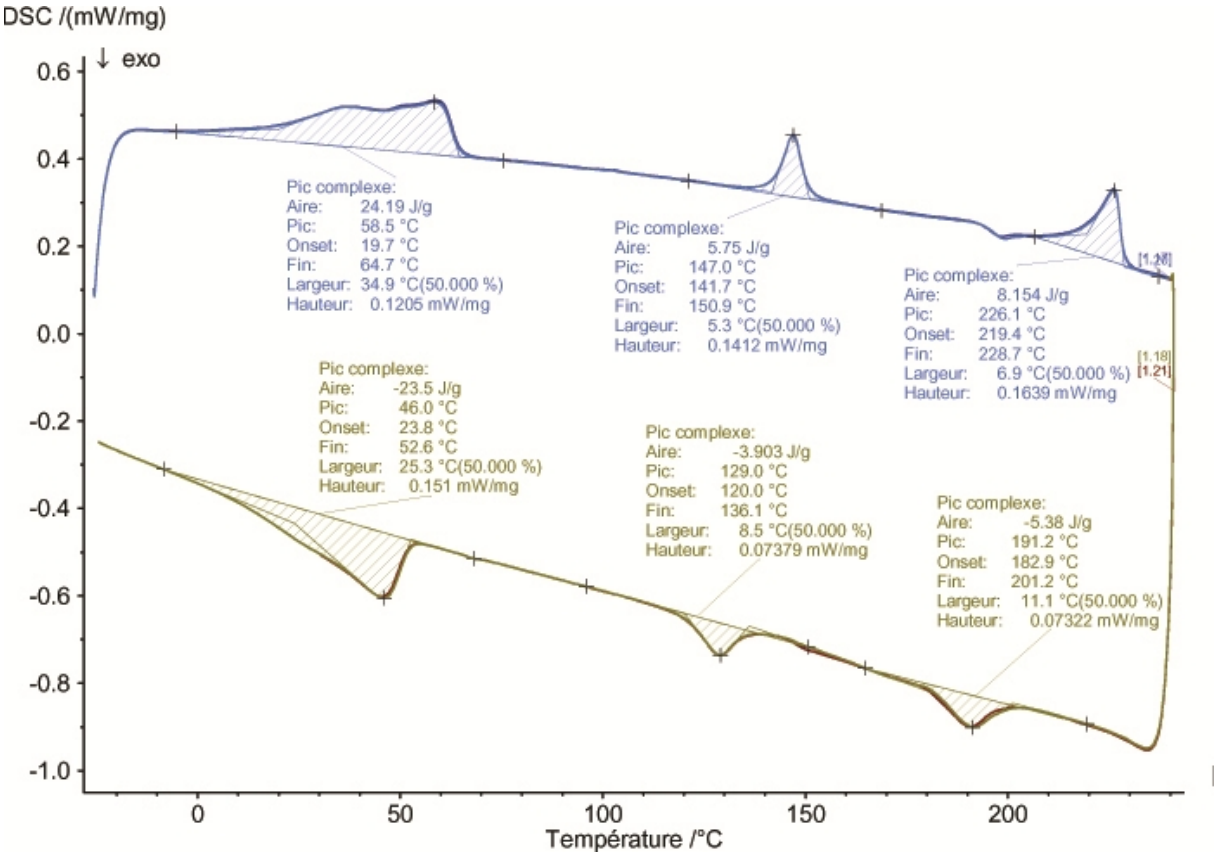


**Figure S3.** DSC traces of compound **1**.

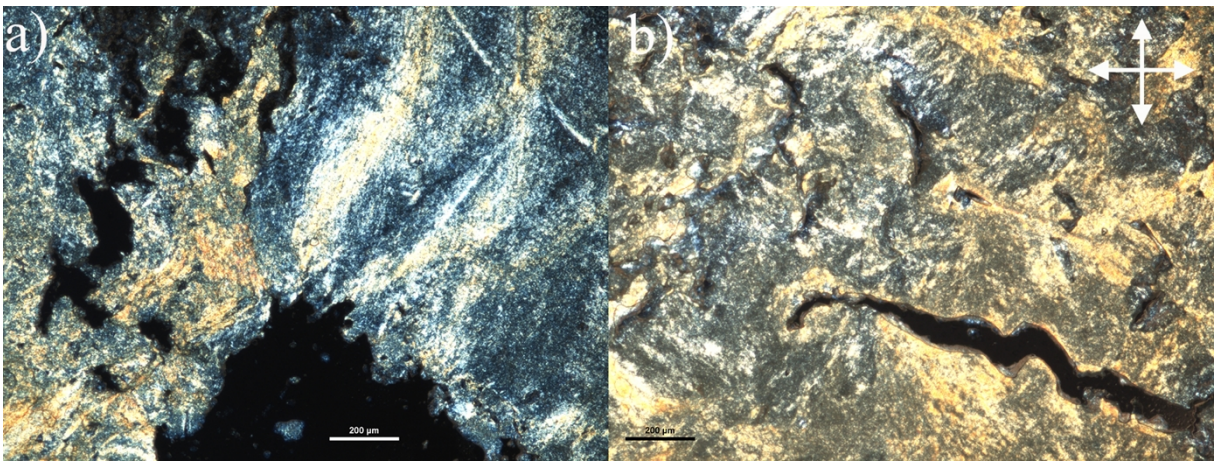


**Figure S4.** Birefringent fluids observed on heating with compound **1** at 190 °C (a) and (b).

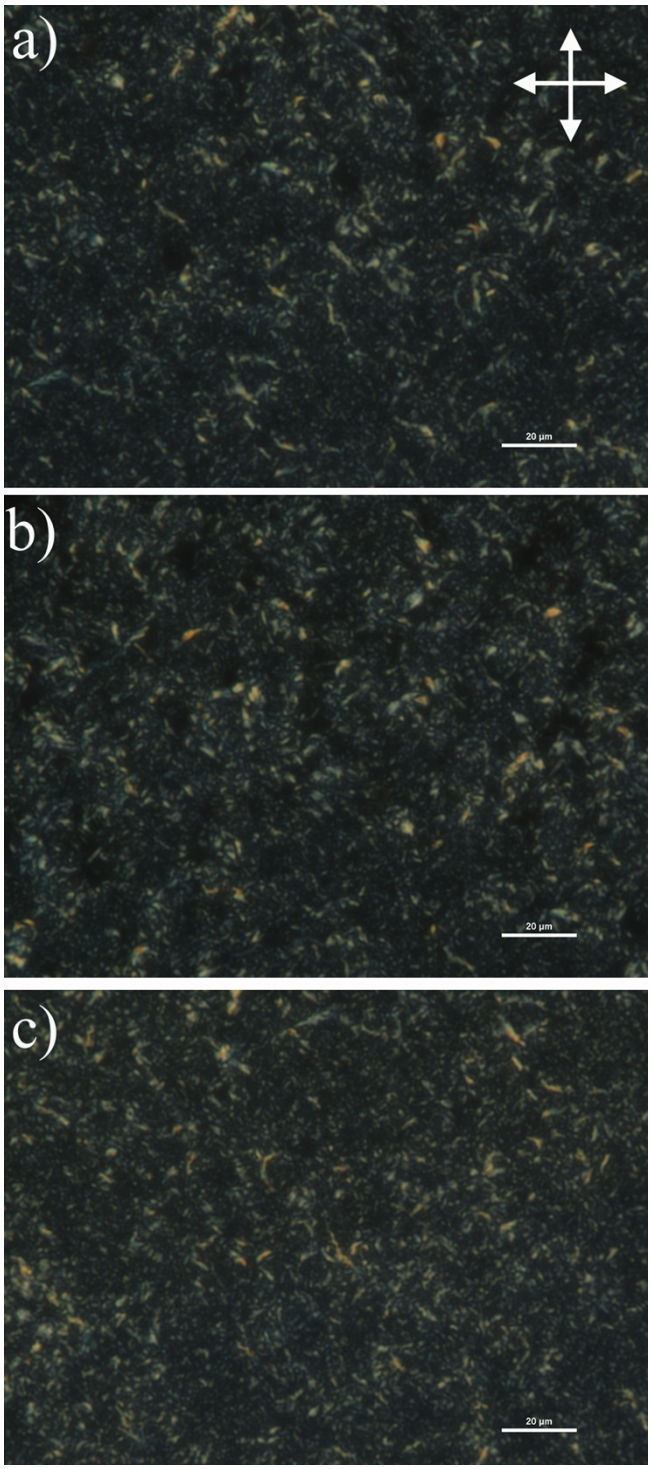


**Figure S5.** Textures observed at 180 °C (a), 80 °C (b) and 25 °C (c).

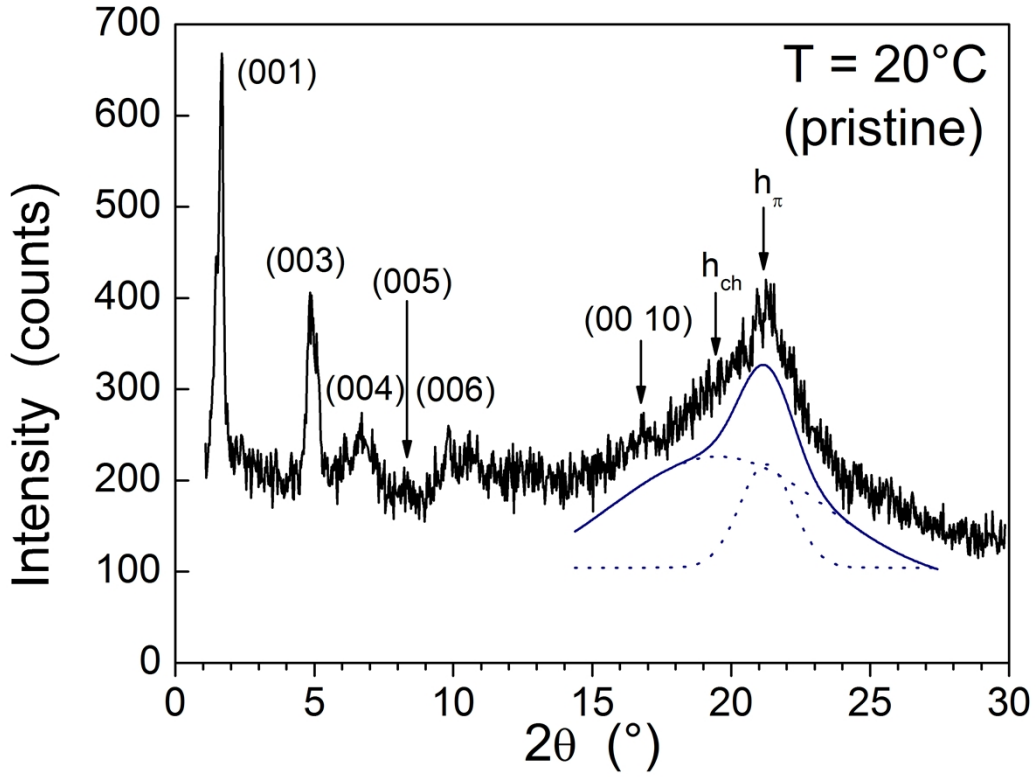


**Figure S6.** X-ray diffractogram of **1**, recorded at 20°C (pristine state)

**Table S2.** Indexation of the reflection of the low-temperature phase of **1** (20°C)

| Peak (00*l*) | $2\theta_{meas.}$[a] (°) | $d_{meas.}$[a] (Å) | Int.[b] (a.u.) | $d_{calc.}$[a] (Å) | $2\theta_{calc.}$[a] (°) | $\Delta 2\theta$[a] (°) |
|---|---|---|---|---|---|---|
| 00*1* | 1.66 | 53.17 | M (sh) | 53.22 | 1.66 | ±0.00 |
| 00*3* | 4.96 | 17.81 | M (sh) | 17.74 | 4.98 | ±0.02 |
| 00*4* | 6.66 | 13.26 | W (sh) | 13.30 | 6.64 | ±0.02 |
| 00*5* | 8.29 | 10.66 | VW (sh) | 10.64 | 8.30 | ±0.01 |
| 00*6* | 9.93 | 8.90 | W (sh) | 8.87 | 9.96 | ±0.03 |
| 00 *10* | 16.72 | 5.30 | VW (sh) | 5.32 | 16.65 | ±0.05 |
| $h_{ch}$ | 19.33 | 4.6 | S (br) | - | - | - |
| $h_{\pi}$ | 21.10 | 4.21 | S (br) | - | - | - |

[a] $\theta_{meas.}$, $\theta_{calc.}$, $d_{meas.}$ and $d_{calc.}$ are measured and calculated diffraction angles and distances. $d_{meas.}$ is obtained from $d_{meas.} = \lambda/(2\sin\theta_{meas.})$, and $d_{calc.}$ is deduced from the following mathematical expression: $d_{00l} = \Sigma N_l.d_{00l}/N_l$, where $N_l$ is the number of 00*l* reflections observed for the lamellar phase, and $2\theta_{calc.} = \arcsin(\lambda/d_{calc.})$; $\Delta 2\theta = \theta_{meas.} - \theta_{calc.}$. [b] VS, S, M, MW, W, VW stand for very strong, strong, medium, medium-weak, weak, very weak and correspond to the reflection intensities; sh and br stand for sharp and broad.

**Table S3.** Indexation of the reflection of the lamellar phase of **1** (80°C)

| Peak (00*l*) | $2\theta_{meas.}$ (°) | $d_{meas.}$ (Å) | Int. (a.u.) | $d_{calc.}$[a] (Å) | $2\theta_{calc.}$ (°) | $\Delta 2\theta$ (°) |
|---|---|---|---|---|---|---|
| 00*1* | 1.63 | 53.77 | VS (sh) | 54.00 | 1.63 | ±0.00 |
| 00*2* | 3.28 | 26.89 | S (sh) | 27.00 | 3.27 | ±0.01 |
| 00*3* | 4.89 | 18.04 | S (sh) | 18.00 | 4.90 | ±0.01 |
| 00*4* | 6.56 | 13.47 | M (sh) | 13.50 | 6.54 | ±0.02 |
| 00*5* | 8.16 | 10.82 | VW (sh) | 10.80 | 8.18 | ±0.02 |
| 00*6* | 9.76 | 9.05 | M (sh) | 9.00 | 9.82 | ±0.06 |
| 00*7* | 11.50 | 7.69 | W (sh) | 7.71 | 11.47 | ±0.03 |
| 00 *10* | 16.43 | 5.39 | M (sh) | 5.40 | 16.40 | ±0.03 |
| $h_{ch}$ | 19.57 | 4.6 | VS (br) | - | - | - |

[a] $\theta_{meas.}$, $\theta_{calc.}$, $d_{meas.}$ and $d_{calc.}$ are measured and calculated diffraction angles and distances. $d_{meas.}$ is obtained from $d_{meas.} = \lambda/(2\sin\theta_{meas.})$, and $d_{calc.}$ is deduced from the following mathematical expression: $d_{00l} = \Sigma\ N_l.d_{00l}/N_l$, where $N_l$ is the number of 00*l* reflections observed for the lamellar phase, and $2\theta_{calc.} = \arcsin(\lambda/d_{calc.})$; $\Delta 2\theta = \theta_{meas.} - \theta_{calc.}$. [b] VS, S, M, MW, W, VW stand for very strong, strong, medium, medium-weak, weak, very weak and correspond to the reflection intensities; sh and br stand for sharp and broad.

**Table S4.** Indexation of the reflection of the rectangular phase of **1** (160°C)

| Peak | $2\theta_{meas.}$ (°) | $d_{meas.}$ (Å) | Int. (a.u.) | Indexation (*hk*) | | $d_{calc.}$ (Å) | $2\theta_{calc.}$ (°) | $\Delta 2\theta$ (°) |
|---|---|---|---|---|---|---|---|---|
| 1 | 1.58 | 55.91 | S (sh) | 20 | 20 | - | - | - |
| 2 | 1.99 | 44.25 | VS (sh) | 11 | 11 | - | - | - |
| 3 | 3.17 | 27.82 | MW (sh) | 40 | 40 | 27.95 | 3.158 | ±0.014 |
| 4 | 3.68 | 23.97 | S (sh) | 02 | 02 | 24.09 | 3.664 | ±0.018 |
| 5 | 3.96 | 22.28 | S (sh) | 22 | 22 | 22.12 | 3.991 | ±0.030 |
| 6 | 4.41 | 20.01 | VW (sh) | 51 | 51 | 20.28 | 4.353 | ±0.058 |
| 7 | 4.78 | 18.47 | S (sh) | 60 | 60 | 18.64 | 4.736 | ±0.045 |
| 8 | 4.90 | 18.01 | S (sh) | 42 | 42 | 18.25 | 4.838 | ±0.062 |
| 9 | 6.01 | 14.68 | M (sh) | 62 | 62 | 14.74 | 5.991 | ±0.022 |
| | | | | 33 | 33 | 14.75 | 5.987 | ±0.026 |
| 10 | 6.38 | 13.84 | M (sh) | 80 | 80 | 13.98 | 6.317 | ±0.063 |
| 11 | 6.70 | 13.18 | W (sh) | 53 | 53 | 13.04 | 6.773 | ±0.073 |
| 12 | 7.29 | 12.11 | W (sh) | 04 | 04 | 12.04 | 7.336 | ±0.046 |
| | | | | 82 | - | 12.09 | 7.305 | ±0.015 |
| | | | | 91 | - | 12.03 | 7.342 | ±0.052 |
| 13 | 8.09 | 10.92 | W (sh) | 44 | 44 | 11.06 | 7.987 | ±0.103 |
| 14 | 8.72 | 10.13 | W (sh) | 10 2 | 10 2 | 10.14 | 8.713 | ±0.004 |
| | | | | 64 | 64 | 10.12 | 8.730 | ±0.013 |
| 15 | 9.21 | 9.59 | W (sh) | 15 | 15 | 9.6 | 9.204 | ±0.006 |
| 16 | 9.85 | 8.97 | S (sh) | 55 | - | 8.84 | 9.997 | ±0.147 |
| | | | | 84 | 84 | 9.12 | 9.690 | ±0.160 |
| 17 | 13.39 | 6.61 | VW (sh) | 57 | 57 | 6.58 | 13.445 | ±0.055 |
| | | | | 10 6 | 10 6 | 6.52 | 13.569 | ±0.179 |
| 18 | 14.66 | 6.04 | M (sh) | 08 | 08 | 6.02 | 14.702 | ±0.042 |

| | | | | | | | | |
|---|---|---|---|---|---|---|---|---|
| | | | | 97 | - | ” | ” | ” |
| 19 | 16.67 | 5.31 | M (sh) | 39<br>10 8 | 39<br>10 8 | 5.30<br>” | 16.713<br>” | ±0.041<br>” |
| 20 | 19.59 | 4.53 | M (sh) | 8 10<br>11 9 | 8 10<br>11 9 | 4.55<br>” | 19.492<br>” | ±0.097<br>” |
| 21 | 21.03 | 4.22 | M (sh) | 12 10 | 12 10 | 4.28 | 20.735 | ±0.299 |
| $h_{ch}$ | 19.30 | 4.6 | VS (br) | - | - | - | - | - |

[a]$d_{calc.}$, a and b are deduced from the following mathematical expression: $1/d_{hk} = \sqrt{(h^2/a^2 + k^2/b^2)}$, and S =a.b, and $S_{col}$ = S/Z. $Col_{rec}$-*c2mm*, a = 111.8(2), b = 48.1(8)Å, Z = 2. Cell area, S: 53878 Å$^2$, column cross-section area, $S_{col}$: 2694 Å$^2$. $V_{mol}$ =4845Å$^3$ (T=160°C). All *hk* follow the conditions *h*+*k* = 2n, centered rectangular lattice *c2mm*. The (*hh*) reflections intensities variation permits to assign the reflection “16” as to (84), the harmonic of the strong reflection (42) rather than to the (55) reflection, which does not follow the regular intensity decrease observed in the series (second indexation column).

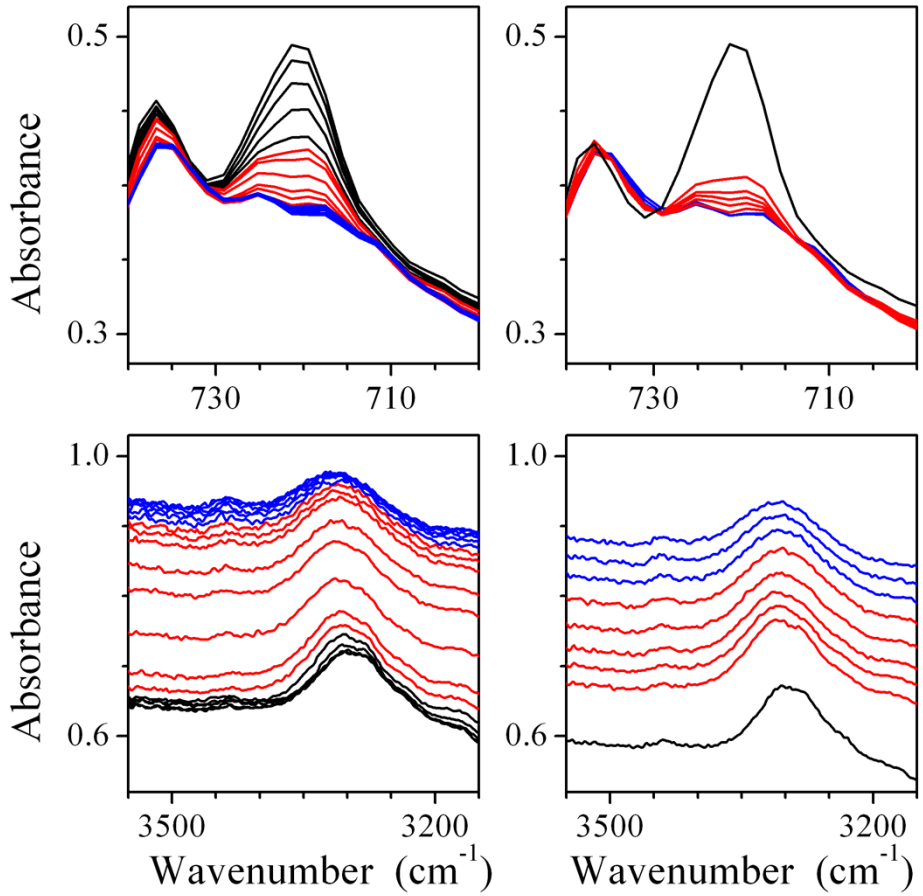


**Figure S7.** IR absorption spectra of compound **1** (2% in KBr pellet) at the following temperatures: 1st heating: 20, 30, 40, 50 and 60°C (room temperature state, black lines), 70, 80, 100, 120, 130, 140, 145 and 150°C (lamellar mesophase, red lines), 155, 160, 165, 170, 175 and 180°C (rectangular mesophase, blue lines); 1st cooling: 160, 150 and 140°C (rectangular mesophase, blue lines), 130, 120, 110, 100 and 80°C (lamellar mesophase, red lines), 20°C (room temperature state, black line). Graphs up: amide V regions with vibration modes of N-H···O bridges; down: N-H stretching regions; left: 1st heating; right: 1st cooling.

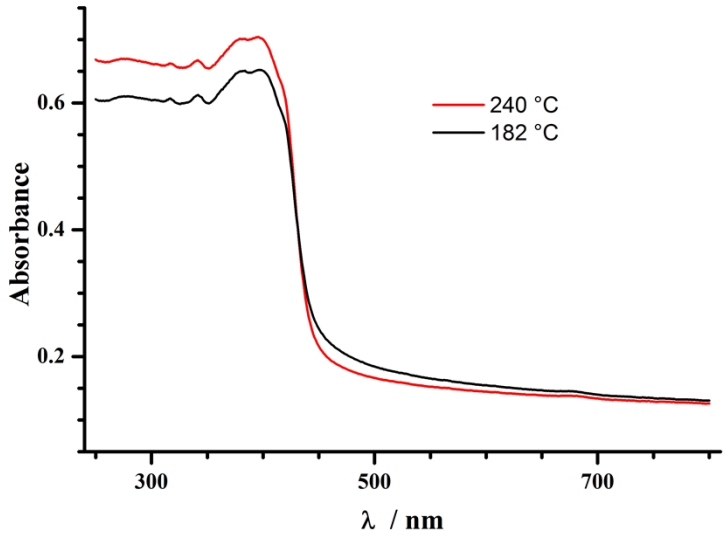


**Figure S8.** Solid-state UV-visible absorption spectra of compound **1** in the isotropic state (240 °C) and in the rectangular mesophase (182 °C).

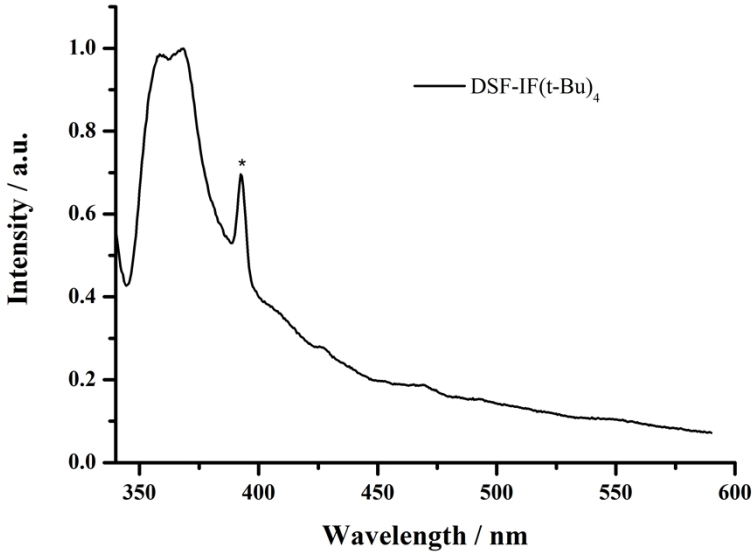


**Figure S9.** Solid-State emission spectra of DSF-IF(t-Bu)$_4$ compound deposited on quartz slide (measured with a PTI spectrofluorimeter) (* = artefact).

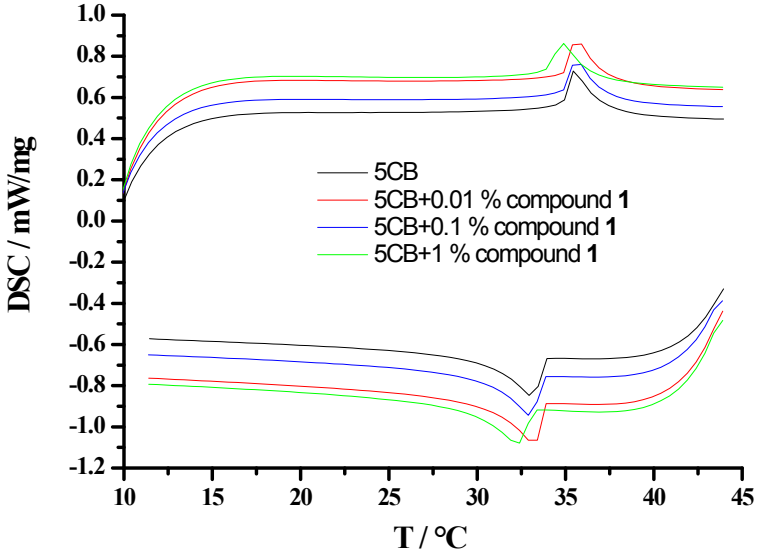


**Figure S10.** DSC traces of 5CB and three mixtures of compound **1**/5CB around the nematic/isotropic transition.